19th Australasian Fluid Mechanics Conference
Melbourne, Australia
8-11 December 2014

Near-wall Electrically Induced Vortices for Quasi-2D MHD Duct Side-wall Heat Transfer Enhancement

Y. Li, A. H. A. Hamid, A. M. Sapardi and G. J. Sheard

Department of Mechanical and Aerospace Engineering
Monash University, Victoria 3800, Australia

Abstract

To enhance the heat transfer from the side-wall of a duct through which an electrically conducting fluid flows within a strong transverse magnetic field, near-wall current injection is introduced as a turbulence generator. An electrode is placed offset from the duct centreline towards the hot wall. Current injected from electrode will radiate and form vortices with the presence of magnetic field, these vortices act to sweep heat from the thermal boundary layer on the hot wall into the duct interior. In this configuration, the flow is quasi-two dimensional and can be solved over a tow-dimensional domain. To maximizing the heat enhancement, Nusselt number is carried out for different setup. Parameters are considered for current strength $1 \leq I \leq 3$, signal frequency $0 < \omega \leq 5$, gap distance $0.2 \leq d \leq 1.0$. The heat enhancement increases with current strength increasing. Maximum heat transfer increment in this study is found to be 18.1% occurring at $I = 3$, $d = 0.67$, $\omega = 1.63$. The pressure drop caused by current induced vortices is within 2% of total pressure drop of the duct which can be neglected.

Introduction

Magnetohydrodynamic flows have been the subject of many investigations during the past few decades because of its practical application in generators, pump, and metallurgical processing. The major application motivating this study is magnetic confinement fusion reactors, where liquid metal is used as a coolant and as a breeder material. In most fusion reactor blankets, the liquid metal circulates in an electrical insulated duct and is heated from the side wall near fusion core. Under strong magnetic field, disturbances in the flow is strongly supressed due to interaction between electrically conducting fluid and magnetic field. Friction from side wall boundary layers parallel to magnetic field, known as Hartmann layer, acts to dampen turbulence. This damping works against the desire to maximise turbulent mixing and convective heat transfer. For a review of liquid-metal flows in magnetic confinement fusion reactor blankets, see [14].

Turbulence promoters is then taken into consideration to invoke convective heat transfer along the heated duct side-wall. Typically used turbulence promoters are cylindrical physical obstacles [4, 7, and 9]. The results reveal that the heat transfer rate under a strong axial magnetic field in insulated ducts was improved by a factor of more than 2 times that of laminar flow. Recent study also shows that the proximity of the cylinder to a wall has a significant influence on the flow and heat transfer characteristics [3]. However, the drawback of employing physical obstacles in the duct is the pressure drop increase, which reduces the overall heat-transfer efficiency [2]. Further, in fusion applications, it may also be impractical to employ complex geometries within the ducts. To overcome these issues, the present study replaces the cylinder with vortices generated by electric current injection from an electrode offset from the duct centreline towards the hot wall. In this configuration, the fluid flows in a duct with three electrically insulated walls where allowing electricity conducting from only one side wall perpendicular to the magnetic field. The bottom wall boundary layers, known as Shercliff layers, are laminar, where heat transfer to it from side wall by conduction. The magnetic field is supposed to be very high that both Hartmann number and the interaction parameter are large.

With high Hartmann number, the MHD damping effect can laminarize the flow so that it can be well described as a quasi-two-dimensional model even for high Reynolds number. Recent three-dimensional simulations at a Reynolds number of 10^5 Shercliff layer laminarized at a Hartmann number of 400 [8]. Research using a Large Eddy Simulation demonstrate that at a Reynolds number of 14,500 turbulence was localized in the Shercliff layers at Hartmann number of 58, but these became fully laminar at a Hartmann number of 65.25 [6].

One of the most proper and commonly used quasi-two-dimensional model for MHD flow is SM82 model which is developed by Sommeria & Moreau [15]. This model is advanced later to allow electromagnetic forces applied on the liquid-metal flow produced by current injection [12]. The analytical model describe nonlinear behaviour of electrically driven circular flow is developed in [13].

The aim of this paper is to establish the relationship between gap current strength, signal frequency, gap distance and heat transfer for quasi-two-dimensional magnetohydrodynamic duct flow.

The paper is organised as follows. The problem is defined in next section, which also presents the governing equations and describes numerical method. Results and discussion section follow after that, with conclusions drawn at last.

Methodology

The geometry of the problem under consideration is shown in Figure 1. A long duct has a uniform rectangular cross section with width $2L$, carrying an electrically conducting fluid. With the duct walls being otherwise electrically insulated, current injected from an electrode embedded in a wall that is perpendicular to the magnetic field will radiate in all directions within the Hartmann boundary layer adjacent to the wall. This leads to an azimuthal acceleration within the boundary layer that in turn acts as a forcing on the two-dimensional core flow. This forcing is strongest at the electrode and decreases with increasing distance from the electrode, generating a vortex at the injection location. By using an appropriately tuned alternating current, a “street” of alternating-sign vortices is created. A strong uniform magnetic field B acts perpendicular to the x-y plane, and an electrode is

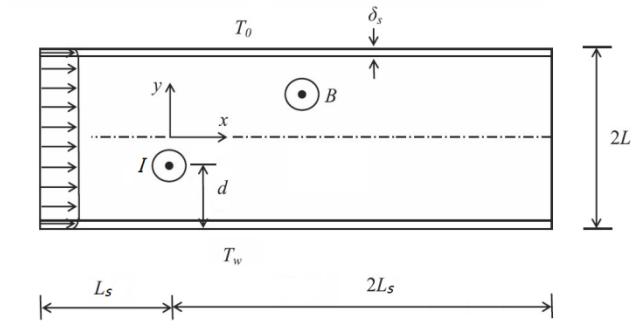

Figure.1. Schematic representation of the system under investigation. The magnetic field *B* acts in the out-of-plane direction. δ_s is the thickness of Shercliff layers. The quasi-2-d. approximation models an out-of-plane channel height of *2a*. The width-to-height aspect ratio *2L/2a* = 1.

placed near the heated bottom wall at distance of *d*. The current-induced vortices are characterized by the gap distance *d*, the current strength *I*, and the frequency ω of signal and the duration of pulse *m*. As described in [15], for a high Hartmann number, the magnetic Reynolds number Re_m, which represents the ratio between the induced and the applied magnetic field is very small and can be neglected. Thus the magnetic field is maintained in z-direction only. Under certain conditions, natural convection may dominant the heat transfer mechanism [1], though this effect is not considered in the present study.

Governing Equations

In this study the non-dimensional MHD equations of continuity, and energy reduced to

$$\nabla \cdot \boldsymbol{u} = 0\,, \tag{1}$$

$$\frac{\partial T}{\partial t} + (\boldsymbol{u}\cdot\nabla)T = \frac{1}{Pe}\nabla^2 T\,. \tag{2}$$

The quasi-two-dimensional momentum equation for an incompressible flow of an electrically conducting fluid between two plates subjected to a uniform strong magnetic field in the out-of-plane direction is given in non-dimensional form by [13]

$$(\partial_t + \boldsymbol{u}\cdot\nabla)\boldsymbol{u} + \nabla p - \frac{N}{Ha^2}\nabla^2\boldsymbol{u} = \frac{N}{Ha}(\boldsymbol{u}_0 - n\boldsymbol{u})\,, \tag{3}$$

where $\boldsymbol{u}$, p and *T* are the pressure, velocity and temperature fields respectively, projected onto the *x-y* plane. The length is scaled by the half duct width *L=a*, pressure by ρU_0^2, where ρ is the density of fluid and U_0 is the peak inlet velocity, time is scaled by a/U_0, and the temperature by the imposed temperature difference between the bottom and top walls, ΔT [1]. The dimensionless parameters Reynolds number *Re*, Peclet number *Pe*, Hartmann number *Ha* and the interaction parameter *N* are defined as

$$Re = \frac{U_0 a}{\nu}, \quad Pe = RePr, \tag{4}$$

$$Ha = aB\sqrt{\frac{\sigma}{\rho\nu}}, \quad N = \frac{\sigma Ba}{\rho u}, \tag{5}$$

where σ and υ are magnetic permeability and kinematic viscosity of the fluid. *Pr* is the Prandtl number, *n* is the number of Hartmann walls. In equation (3), $\boldsymbol{u_0}$ is the force vector field, and is defined as

$$\boldsymbol{u}_0 = \boldsymbol{j}\times\boldsymbol{e}_z\,, \tag{6}$$

At low electrical resistance, Ohm's law is linear. The equations governing continuity of electric current and incompressibility are also linear so they may be averaged to give $\nabla\cdot\boldsymbol{j} = j_w$ and $\frac{1}{Ha}\boldsymbol{j} = E + \boldsymbol{u}\times\boldsymbol{e_z}$ and equation (1). Here j_w is the current density injected at one or both of the confining planes, *E* is a dimensionless electric field.

The *z*-averaged current can be expressed as the gradient of a scalar ψ_0 satisfying a Poisson equation with the source term being j_w as $\boldsymbol{j} = \nabla\psi_0, \nabla^2\cdot\psi_0 = -j_w$ [13]. Solve this Poisson equation for a source term at current injection point that is a Dirac function located at $\mathbf{x} = (0, d)$, i.e. $\Phi(x,y) = j_w(x,y) = I\delta(x, y-d)$, on a domain extending infinitely in streamwise direction and bounded by duct side-walls. Imposing Neumann condition at the boundaries due to insulating Shercliff walls [12], i.e. $\frac{\partial\psi_0}{\partial z} = 0$ at $y = -L$ and $y = L$, leads to

$$\psi_0(x,y) = \frac{I}{4\pi}\left[\ln\frac{1}{\cosh(\pi x/2L) - \cos[\pi(y+L-d)/2L]} + \ln\frac{1}{\cosh(\pi x/2L) - \cos[\pi(y+L+d)/2L]}\right]. \tag{7}$$

The solving of this Poisson equation can be found on [11]. *I* is the current amplitude which is non-dimensionalized as

$$\hat{I} = IaU_0\sqrt{\rho\nu\sigma} = I\cdot Re\sqrt{\rho\nu^3\sigma}\,. \tag{8}$$

Substitute equation (7) into equation (6), the force field becomes

$$\boldsymbol{u}_0 = \nabla\psi_0\times e_z = \left\langle\frac{\partial w}{\partial x}, \frac{\partial w}{\partial y}, 0\right\rangle\times e_z\,. \tag{9}$$

The local Nusselt number along the bottom heated wall of the channel is defined as

$$Nu_w(x,t) = \frac{a}{(T_f - T_w)}\frac{\partial T}{\partial y}\Big|_{wall}\,, \tag{10}$$

T_f is the bulk fluid temperature, which is calculated using the velocity and temperature distribution as

$$T_f(x,t) = \int_0^{2L} uT dy \Big/ \int_0^{2L} u dy\,, \tag{11}$$

A time-averaged Nusselt number for heat transfer through the heated wall of the channel is calculated by first take the time average of the local Nusselt number ($\overline{Nu_w}$) at each x-station, and then integrating over the length of the heated bottom wall, $3L_s$

$$Nu = \frac{1}{3L_s}\int_0^{3L_s}\overline{Nu_w}(x)dx\,, \tag{12}$$

To characterize the effect on the heat transfer due to the addition of current injection to the channel, the overall increment of heat transfer is defined as (in percentage)

$$HI = (Nu - Nu_0)\big/Nu_0\times 100\,, \tag{13}$$

where Nu_0 is the time-average Nusselt number of the heated region of the duct without any turbulence promoter.

Numerical Methods

A nodal spectral-element method is utilized to discretise the governing flow and energy equation in space. The setup of the system is similar as in [3]. The meshes are generated based on meshing empty channel while condense at current injection point.

A no-slip boundary condition for velocity is imposed on all solid walls. At the channel inlet, a normal component of velocity is assumed to be zero, and a Hartmann velocity profile for the axial velocity is applied. At the exit, a constant reference pressure is imposed.

A grid resolution study determined the computational domain size, number of mesh elements and the required number of nodes per element to resolve the flow features to within 1%. The

meshes comprise 876 macro elements with 36 (6×6) nodes per element.

The present study uses a step current signal with an alternating pulse waveform. The duration of the pulses is 25m% of time period of signal and the period of signal is $2\pi/\omega$. To obtain a stable vortex shedding, duration of pulse m is set as constant 2. Prandtl number 0.022 equivalent to eutectic liquid-metal alloys at room temperature is used for simulation.

Results and Discussion

To demonstrate the interaction of the wall boundary layers and current induced vortices, a Reynolds number of 1500 and a Hartmann number of 500 are chosen. Figure 1 shows the different dynamics of the flow with varies parameters. First of all, the heat transfer enhancement is influenced by two main factors. One is the "bouncing up" effect of vortex shedding which carry high energy flow from bottom wall to centre of channel. Another is the space between each pair of vortices, which provide a "passage" for high energy flow to be "sucked up". The gap distance d has most effect on vortex shedding. From figure 1 (a) to (c), it can be observed that the distance between each vortex decreases with gap distance. While current injection point is placed closer to bottom wall, the interaction between bottom wall and vortices becomes stronger. However the space between two vortices disappears. Due to significant flow velocity difference, the anti-clockwise vortex drives flow into Shercliff layer and moves slower, while clockwise vortex drive flow out from Shercliff layer to upper layer and moves faster, the two vortices then collide (figure 1 (c)). This means the energy of vortices is contribute not only to spin the flow, but also to push each other. For above reason, it is preferred to place electrode slightly far from the wall as shown in figure 1 (b).

Figure 1 (c) and (d) shows effect of signal frequency influencing the vortex growth. The lower the frequency, the longer time period that Lorentz force acting on the flow, the vortex grow larger. Amplitude play a simple role in current injection as can be seen in figure 1 (d) and (e). Lower the amplitude, smaller the Lorentz force, weaker the interaction between bottom wall and wakes will be. Increase current strength will increase the speed of energy "charging" into vortices.

In order to characterize the effect of vortex patterns on the wall heat transfer, instantaneous temperature plots accompany the vorticity plots are present in figure2. It will be show later that for gap distance d=0.6, the heat transfer increases markedly.

Figure 3 presents two series of sample data based on Nusselt number verses signal frequency. Notice that for small gap distance, its Nusselt number plot has two local peak, which is possibly due to different signal response modes. With d increases, this effect vanishes. As the frequency rises from zero plus to 1, the Nusselt number increases substantially. In most cases except small gap distance, the peak Nusselt number is located between ω=1 and ω=2. Further increasing signal frequency will cause a drop on Nusselt number. For high current amplitude, heat transfer drops more steeply. Note the dashed line in figure 3 means Nu_0 which is for an empty channel without any vortex generator.

The pressure drop increment due to obstacle vortex promoter is usually from 5% to 60% [4]. However for current injection, it is only between 0.3% and 1.5%. Which means the pressure drop heat enhancement penalty can be neglect.

As shown in figure 3, all plots have global peaks which is picked to illustrate the relationship between Nu peak and gap distance. It is presented in figure 4 (a). These plots show trends on how maximizing heat transfer is related with gap distance. It also indicates that peak heat transfer enhancement occur around d=0.65, with slightly difference (within 0.04) for different

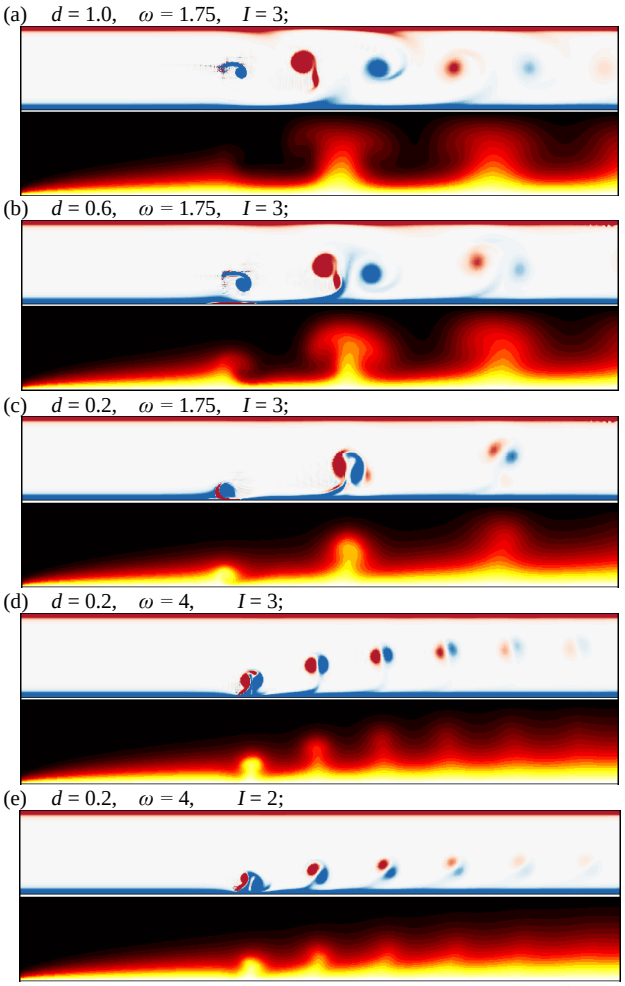

Figure 2. Contour plots of vortex shedding and temperature field for different parameters. These contours are arranged by varying one parameter: (a) to (c), decrease d; (c) to (d) increase ω; (d) to (e) decrease I.

current amplitude. As present results indicate, the heat enhancement and amplitude are in a power relationship.

The figure 4 (b) represent the different signal frequency where all these peak heat enhancement are find. As can be expected from figure 3 (a), at small gap distance the peak frequencies vary a lot since different modes of response occur. From d=0.55 to d=0.8, these frequencies show a consistency around 1.6. Since the main concern is about maximizing heat transfer, at current stage this study only consider peak occur at d around 0.65.

To judge the applicability of this study, the non-dimensional current amplitude is dimensionalized using equation (8). For experimental used low-melting eutectic alloy $Ga^{68}In^{20}Sn^{12}$, which has the following properties: density $\rho = 6.36\times10^3$ kgm^{-3}, electrical conductivity $\sigma = 3.46 \times 10^6$ Ω^{-1}m^{-1} and kinematic viscosity $\nu = 3.40 \times 10^{-7}$ m^{2}s^{-1} [6], the non-dimensional current I = 3 represents a current of 0.1323 Ampere at Reynolds number equals to 1500. It is easily achievable in real applications.

Conclusions

An investigation has been carried out into characteristics of MHD flow and heat transfer enhancement with current injection placed offset from the duct centreline using spectral-element method. For these conditions, the flow is quasi-two-dimensional and the modified Navier-Stokes equations are solved in a two-dimensional domain. The numerical simulations have been performed for fixed Reynolds number Re=1500, current strength $1 \le I \le 3$, signal frequency $0 < \omega \le 5$, gap distance $0.2 \le d \le 1.0$ and constant Hartmann number Ha=500.

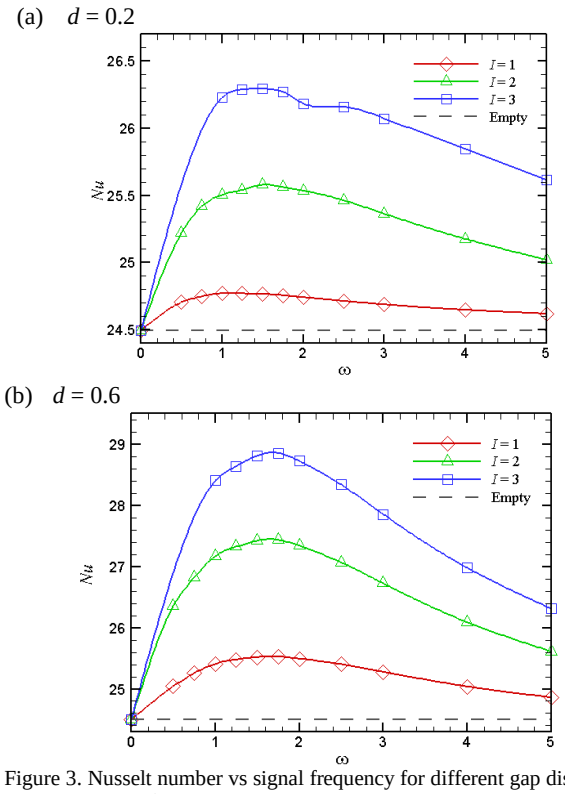

Figure 3. Nusselt number vs signal frequency for different gap distance *d*. Current strength from 1 to 3 is tested. Empty means Nu_0 described before.

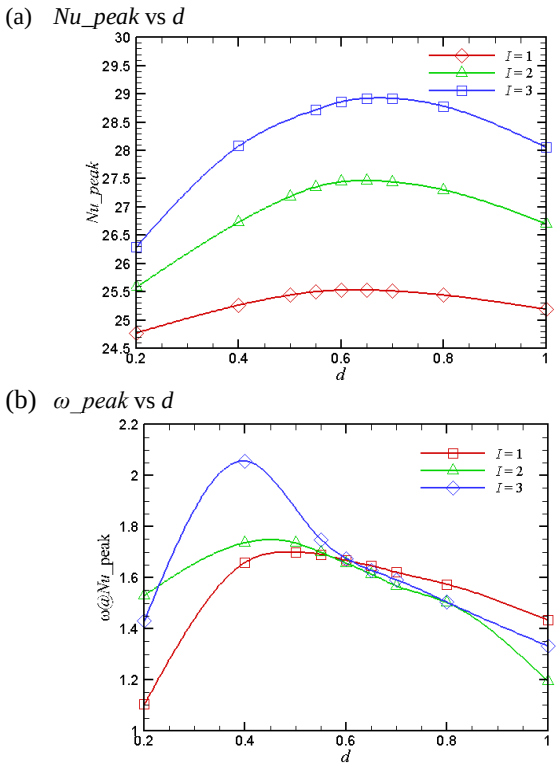

Figure 4. All peak Nusselt number as can be seen in figure (3) are picked and plotted against gap distance in (a). Frequencies at these peaks are also plotted against *d* which is shown in (b)

The results show that for current injection point offset from centreline, the vortex street drifts further away from the wall and convects downstream. Heat enhancement is proportional to current amplitude. It is also significantly influenced by signal frequency. The Nusselt number rapidly rises with frequency increase, reaches peak around ω = 2, then drops with further frequency ascension. At small gap distance, the responses of signal frequency become complicated with different modes.

To maximize the heat enhancement, the best setup is found at gap distance from 0.63 to 0.67 for current amplitude from 1 to 3. The maximum heat transfer increment *HI* for *I*=3 is recorded to be 17%. The pressure drop caused by induced vortices is significant small which can be neglect. That means no pressure drop penalty on heat transfer occurs for current injection method.

Acknowledgments

This research was supported by ARC Discovery Grant DP120100153, high-performance computing time allocations from the National Computational Infrastructure (NCI) and the Victorian Life Sciences Computation Initiative (VLSCI), and the Monash SunGRID.

References

[1] Barleon L., Burr U., MacK K.-J., & Stieglitz R., Heat transfer in liquid metal cooled fusion blankets, *Fusion Eng. Des.* **51–52**, 2000, 723–733.

[2] Hussam W.K., Thompson M.C. & Sheard, G.J., Dynamics and heat transfer in a quasi-two-dimensional MHD flow past a circular cylinder in a duct at high Hartmann number, *International Journal of Heat and Mass Transfer* **54 (5)**, 2011, 1091-1100.

[3] Hussam W. K., Sheard G. J., Heat transfer in a high Hartmann number MHD duct flow with a circular cylinder placed near the heated side-wall, *International Journal of Heat and Mass Transfer* **67**, 2013, 944–954.

[4] Hussam W.K., Thompson M.C. & Sheard, G.J., Enhancing heat transfer in a high Hartmann number magnetohydrodynamic channel flow via torsional oscillation of a cylindrical obstacle, *Phys. Fluids* **24**, 2012, 113601.

[5] Jian D. and Karcher C., Electromagnetic flow measurements in liquid metals using time-of-flight Lorentz force velocimetry, *Meas. Sci. Technol.* **23**, 2012, 074021.

[6] Kobayashi H., Large eddy simulation of magneto-hydrodynamic turbulent duct flows, *Phys. Fluids* **20**, 2008, 015102.

[7] Kolesnikov Y. B. & Tsinober A. B., Two-dimensional turbulent flow behind a circular cylinder, *Magn. Gidrodin.* **8 (3)**, 1972, 23–31. English translation: *Magneto-hydrodynamics* **8 (3)**, 1972, 300–307.

[8] Kolesnikov Y. B. & Andreev O.V., Heat-transfer intensification promoted by vortical structures in closed channel under magnetic field, *Experimental Thermal and Fluid Science* **15 (2)** , 1997, 82–90.

[9] Krasnov D., Zikanov O. & Boeck T., Numerical study of magnetohydrodynamic duct flow at high Reynolds and Hartmann numbers, *J. Fluid Mech.* **704**, 2012, 421–446.

[10] Moreau J. & Sommeria R., Electrically driven vortices in a strong magnetic field, *J.Fluid Mech.* **189**, 1988, 553–569.

[11] Polyanin A. D., *HANDBOOK OF LINEAR PARTIAL DIFFERENTIAL EQUATIONS for ENGINEERS and SCIENTISTS*, CRC Press Company, 2002, 490-513.

[12] Pothérat A., Sommeria J. & Moreau R., An effective two-dimensional model for MHD flows with transverse magnetic field. *J. Fluid Mech.*, **424**, 2000, 75-100.

[13] Pothérat A., Sommeria J. & Moreau R., Numerical simulations of an effective two-dimensional model for flows with a transverse magnetic field. *J. Fluid Mech.*, **534**, 2005, 115-143.

[14] Smolentsev S., Moreau R., Bühler L. & Mistrangelo C., MHD thermofluid issues of liquid-metal blankets: phenomena and advances, *Fusion Eng. Des.* **85**, 2010, 1196–1205.

[15] Sommeria J. & Moreau R., Why, how, and when, MHD turbulence becomes two-dimensional, *J.Fluid Mech.* **118**, 1982, 507–518.

[16] Yang S.-J., Numerical study of heat transfer enhancement in a channel flow using an oscillating vortex generator, Heat Mass Transfer **39**, 2003, 257–26.